

Structure of single- Λ hypernuclei with chiral hyperon-nucleon potentials

Johann Haidenbauer¹ and Isaac Vidaña²

¹Institute for Advanced Simulation, Institut für Kernphysik (Theorie) and Jülich Center for Hadron Physics, Forschungszentrum Jülich, D-52425 Jülich, Germany

²Istituto Nazionale di Fisica Nucleare, Sezione di Catania. Dipartimento di Fisica “Ettore Majorana”, Università di Catania, Via Santa Sofia 64, I-95123 Catania, Italy

Received: date / Revised version: date

Abstract. The structure of single- Λ hypernuclei is studied using the chiral hyperon-nucleon potentials derived at leading order (LO) and next-to-leading order (NLO) by the Jülich–Bonn–Munich group. Results for the separation energies of Λ single-particle states for various hypernuclei from ${}^5_\Lambda\text{He}$ to ${}^{209}_\Lambda\text{Pb}$ are presented for the LO interaction and the 2013 (NLO13) and 2019 (NLO19) versions of the NLO potentials. It is found that the results based on the LO potential show a clear tendency for overbinding while those for the NLO13 interaction underbind most of the considered hypernuclei. A qualitatively good agreement with the data is obtained for the NLO19 interaction over a fairly large range of mass number values when considering the uncertainty due to the regulator dependence. A small spin-orbit splitting of the p -, d -, f -, and g -wave states is predicted by all interactions, in line with the rather small values observed in pertinent experiments.

PACS. 13.75.Ev Hyperon-nucleon interactions – 21.80.+a Hypernuclei – 21.30.Fe Forces in hadronic systems and effective interactions

1 Introduction

One of the goals of hypernuclear physics [1–3] is to relate hypernuclei observables with the underlying bare hyperon-nucleon (YN) and hyperon-hyperon (YY) interactions which, contrary to that between two nucleons (NN), are still poorly known due to the limited number and accuracy of scattering data [4–7]. Hypernuclei, therefore, constitute a valuable and complementary source of information to constrain better these interactions. In a simple picture, single- Λ hypernuclei consist of an ordinary nucleus with the Λ hyperon sitting in a single-particle state of an effective Λ -nucleus mean field potential. Based on this description, several approaches have been employed to study the properties of the Λ hyperon in finite nuclei. Woods-Saxon potentials, for instance, have been traditionally used to describe, in a shell model picture, the single-particle properties of the Λ from medium to heavy hypernuclei [8–11]. Density dependent effects and non-localities have been included in non-relativistic Hartree-Fock calculations with Skyrme type YN interactions in order to improve the overall fit of the single-particle energies [12–20]. The properties of hypernuclei have also been studied in a relativistic framework, such as Dirac phenomenology, where the hyperon-nucleus potential is derived from the nucleon-nucleus one [21, 22], or from relativistic mean field theory [23–33]. Microscopic hypernuclear structure

calculations, which can provide the desired link between the hypernuclear observables and the bare YN interaction, are also available. In these calculations the single-particle properties of the Λ in the hypernucleus have been mostly derived from effective YN G -matrices built from bare YN interactions [34–41]. Recently, a quantum Monte Carlo calculation of single- and double- Λ hypernuclei has been done using two- and three-body forces between the Λ and the nucleons [42, 43]. In most of these approaches, the quality of the description of hypernuclei relies on the validity of the mean field picture. However, the correlations induced by the YN interaction can substantially change this picture and, therefore, should not be ignored a priori. Very recently, the spectral function of the Λ in finite nuclei has been studied by one of the authors of the present work [44], showing that the Λ is less correlated than the nucleons in agreement with the idea that it maintains its identity inside the nucleus. The results of this study show also that in hypernuclear production reactions the Λ hyperon is formed mostly in a quasi-free state.

Microscopic calculations of hypernuclear structure are usually based on realistic YN interactions that describe the available scattering data in free space. These interactions have been mainly constructed within the framework of a meson-exchange theory [45–52]. In recent years, however, YN interactions have been also derived in $SU(3)$

chiral effective field theory (χ EFT) by the Jülich–Bonn–Munich group, first at leading order (LO) [53] and, then, at next-to-leading order (NLO) in the Weinberg power counting [54, 55]. The LO potential consists of four-baryon contact terms without derivatives and of one-pseudoscalar-meson exchanges whereas at NLO contact terms with two derivatives arise together with loop contributions from (irreducible) two-pseudoscalar-meson exchanges (see Fig. 1 of Ref. [54]). Corresponding and consistent hyperon-nucleon-nucleon (YNN) interactions have been likewise derived by the Jülich–Bonn–Munich group in χ EFT [56]. The leading contributions, consisting of three-body forces (3BFs) due to two-meson exchange, one-meson exchange, and six-baryon contact terms, appear at next-to-next-to-leading order (N^2 LO) in the applied Weinberg counting.

In the present work we examine the chiral LO and NLO YN interactions [53–55] in microscopic hypernuclear-structure calculations. So far, these YN potentials from chiral EFT have been employed only in studies of light hypernuclei [55, 57–62], and of the properties of hyperons in (infinite) nuclear matter [63–67] using the Brueckner–Hartree–Fock (BHF) approach. For instance, in Ref. [66], it was found that the Λ single-particle potential at zero momentum in symmetric nuclear matter and pure neutron matter becomes repulsive for densities larger than about two times normal nuclear saturation density, in contrast with the results obtained in similar BHF calculations with more conventional meson-exchange potentials. From this result, the authors of Ref. [66] concluded that in neutron star matter this repulsion would shift the onset of hyperons to high densities potentially solving the so-called “hyperon puzzle”, *i.e.*, the difficulty to reconcile the recent observation of $2M_\odot$ neutron stars with the presence of hyperons in their interiors (see *e.g.*, Ref. [68] and references therein).

Faddeev-type calculations of the hypertriton, ${}^3_\Lambda\text{H}$, performed with the LO [57] and NLO [55] interactions, yield a satisfactory value for the separation energy. However, one should keep in mind that this energy has been actually used as an additional constraint for fixing the relative strength of the singlet- and triplet ΛN S -wave interactions [53–55]. Calculations of the separation energies for the four-body hypernuclei ${}^4_\Lambda\text{H}$ and ${}^4_\Lambda\text{He}$ based on the EFT interactions revealed that there is only a qualitative agreement with the experiments [55, 57]. Specifically, the 0^+ state is slightly overbound by the LO interaction [57] and noticeably underbound by the NLO interactions [55]. For fairness one has to say that an underbinding is likewise observed for phenomenological models of the YN interaction [55]. The LO interaction has been also used in studies of light hypernuclei from ${}^4_\Lambda\text{H}/{}^4_\Lambda\text{He}$ to ${}^{13}_\Lambda\text{C}$ in *ab initio* calculations based on the no-core shell model (NCSM) [58–62] and corresponding results for the NLO interaction are becoming available too [69, 70].

The manuscript is organized in the following way. In Sec. 2 we briefly describe the method to obtain the Λ single-particle properties in finite nuclei. Results for a variety of single- Λ hypernuclei are shown in Sec. 3. Finally,

a brief summary and some concluding remarks are given in Sec. 4.

2 Λ single-particle properties in finite nuclei

The aim of this work is to study the properties of the Λ in several nuclei using the chiral YN interactions of the Jülich–Bonn–Munich group at LO and NLO. We follow a perturbative many-body approach to calculate the Λ self-energy in finite nuclei from which we can determine the different Λ single-particle bound states in the corresponding hypernuclei under study. This approach was originally developed to study the properties of the nucleon [71] and the Δ [72] isobar in finite nuclei, and has been already extended to study those of the Λ and Σ hyperons in Refs. [40, 41, 44] using meson-exchange YN interactions. In the following we present a brief summary of this approach and refer the interested reader to Refs. [40, 41, 44, 71, 72] for a detailed description. The approach starts with the construction of all the YN G -matrices which describe the interaction between a hyperon ($Y=\Lambda, \Sigma$) and a nucleon in infinite nuclear matter. To such end the coupled-channel Bethe–Goldstone equation is solved in momentum space including partial waves up to a maximum value of the total angular momentum $J = 4$. We note here that, when solving it, the so-called discontinuous prescription has been adopted. These G -matrices are then used to obtain the YN G -matrices in finite nuclei through the following integral equation:

$$\begin{aligned} G_{FN} &= G + G \left[\left(\frac{Q}{E} \right)_{FN} - \left(\frac{Q}{E} \right) \right] G_{FN} \\ &= G + G \left[\left(\frac{Q}{E} \right)_{FN} - \left(\frac{Q}{E} \right) \right] G \\ &\quad + G \left[\left(\frac{Q}{E} \right)_{FN} - \left(\frac{Q}{E} \right) \right] G \left[\left(\frac{Q}{E} \right)_{FN} - \left(\frac{Q}{E} \right) \right] G \\ &\quad + \dots, \end{aligned} \quad (1)$$

which expresses the finite nuclei G -matrices, G_{FN} , in terms of the nuclear matter ones, G , and the difference between the finite-nucleus and the nuclear-matter propagators, written schematically as $(Q/E)_{FN} - (Q/E)$. This difference, which accounts for the relevant intermediate particle-particle states has been shown to be quite small [40, 41, 44, 71, 72] and, thus, in all practical calculations G_{FN} can be well approximated by truncating the expansion (1) up to second order in the nuclear matter G -matrices. Therefore, we have

$$G_{FN} \approx G + G \left[\left(\frac{Q}{E} \right)_{FN} - \left(\frac{Q}{E} \right) \right] G. \quad (2)$$

Using then G_{FN} as an effective YN interaction we obtain the Λ self-energy in the BHF approximation (see diagram (a) of Fig. 1). This approximation can be split into the sum of two contributions: the one shown by diagram (b), which originates from the first-order term on the right-hand side of Eq. (2), and that of diagram (c), which stands for the so-called *two-particle-one-hole* (2p1h)

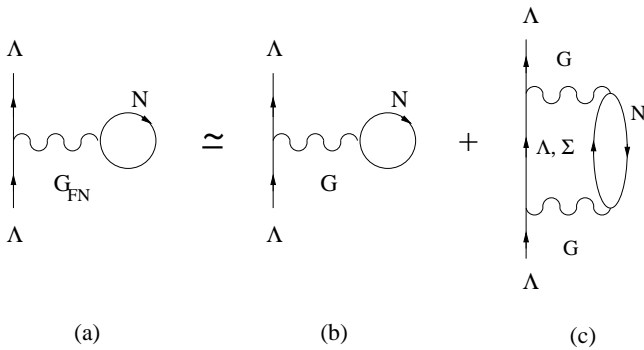


Fig. 1. BHF approximation of the finite nucleus Λ self-energy (diagram (a)), split into the sum of a first-order contribution (diagram (b)) and a second order 2p1h correction (diagram (c)).

correction, where the intermediate particle-particle propagator has to be viewed as the difference of propagators appearing in Eq. (2). Solving the Schrödinger equation with the real part of the Λ self-energy we are able to determine, as we just mentioned, the different Λ single-particle bound states.

Before we present and analyze our results in detail, we would like to point out a particular feature of the employed method that will be of relevance below. The distortion of the plane wave associated with the nucleon in the intermediate state of the 2p1h diagram of Fig. 1(c), necessary to ensure its orthogonalization to the nucleon hole states, is taken into account only approximately. The orthogonalization procedure, described in detail in Ref. [71], was originally optimized for the case of $^{17}_{\Lambda}\text{O}$ [40]. As a consequence, the method tends to overestimate the binding energies for very heavy hypernuclei such as $^{91}_{\Lambda}\text{Zr}$ and $^{209}_{\Lambda}\text{Pb}$. Indeed, as discussed already in Refs. [41, 44], and as we will see below, in general it leads to results where the Λ is more bound in those nuclei than in infinite nuclear matter. This, of course, represents a clear signal for limitations in the applicability of that method to the heaviest hypernuclei.

3 Results and discussion

The separation energies of the different Λ single-particle states in $^5_{\Lambda}\text{He}$, $^{13}_{\Lambda}\text{C}$, $^{17}_{\Lambda}\text{O}$, $^{41}_{\Lambda}\text{Ca}$, $^{91}_{\Lambda}\text{Zr}$ and $^{209}_{\Lambda}\text{Pb}$ obtained with the chiral interactions are summarized in Table 1. Note that all hypernuclei considered in the present work consist of a closed-shell nuclear core plus a Λ sitting in a single-particle state. The values reported are to be compared with the experimental separation energies for the corresponding hypernuclei. However, since experimental data for the particular hypernuclei we consider do not always exist, we include for comparison the closest representative hypernuclei for which experimental information is available. However, one should not attribute the differences between the calculated and the experimental values to this fact. These are mainly due to the approximative

character of the calculation and/or, of course, due to the properties of the employed YN interactions.

Results are presented for the LO interaction from 2006 [53] and the two NLO versions from 2013 (NLO13) [54] and 2019 (NLO19) [55]. The latter interactions differ by different choices for the low-energy constants (LECs) that determine the strength of the contact interactions. In the initial NLO potential published in 2013 [54] all LECs in the S -waves were fixed by a fit to the available Λp and ΣN data at low energies. In the NLO19 potential some of the S -wave LECs were inferred from the NN sector via the underlying SU(3) flavor symmetry so that only a reduced number of LECs needed to be determined from the empirical information in the YN sector, see Ref. [55] for details. The interaction in the P -waves and in higher partial waves is the same in the two potentials. As discussed thoroughly in Ref. [55] the results for Λp and ΣN scattering observables for the NLO13 and NLO19 potentials are practically identical. However, there is a considerable difference in the strength of the $\Lambda N \rightarrow \Sigma N$ transition potential between the two interactions and that has an influence on few- and many-body applications like the one in the present work.

Chiral baryon-baryon interactions derived within the Weinberg scheme require a regularization when inserted into the scattering (Lippmann-Schwinger) or G -matrix (Bethe-Goldstone) equations [75]. As a consequence, the results depend on the regulator, specifically on the cutoff mass Λ in the exponential regulator function adopted in the chiral YN potentials of the Jülich-Bonn-Munich group [53–55]. Since, in principle, observables should not depend on the regulator, the actual regulator dependence provides arguably a measure for the magnitude of (missing) higher order contributions to the YN interaction, and in case of applications to few- and many-body systems also for missing many-body forces, in particular of 3BFs [57, 76]. Accordingly, the results for the chiral interactions in Table 1 are given for a range of cutoff masses. The variation with the cutoff has to be considered as a lower bound for the uncertainty due to truncation of the chiral expansion. The range chosen for Λ is similar to what was used for chiral NN potentials [75]. The actual values, $\Lambda = 550\text{--}700$ MeV (for the LO interaction) and $\Lambda = 500\text{--}650$ MeV (NLO), correspond to the range where the best description (lowest χ^2) of Λp and ΣN scattering data was achieved [54, 55]. NLO results for the cutoff $\Lambda = 700$ MeV are included here for reasons discussed below.

We want to emphasize that no modifications of the underlying YN interactions are applied in the course of our calculation to improve the description of hypernuclei.

Let us analyze the results now. Interestingly, there is a rather good agreement between experimental data and the results obtained with the LO chiral YN interaction for $^5_{\Lambda}\text{He}$ and $^{13}_{\Lambda}\text{C}$ in the whole range of cutoff values. However, it is informative to compare our predictions for these two hypernuclei with the ones of a recent *ab initio* calculation based on the NCSM by Wirth and Roth [62] where likewise this LO YN potential was employed. In principle, the latter calculation should yield “exact” results when fully converged. (NCSM results for $^4_{\Lambda}\text{He}$ [60, 61] based on the

Λ (MeV)	LO				NLO13					NLO19					Exp.
	550	600	650	700	500	550	600	650	700	500	550	600	650	700	
${}^5_{\Lambda}\text{He}$ $s_{1/2}$	4.04	3.32	3.06	3.26	0.73	0.15	0.63	2.36	4.90	2.16	1.36	1.77	3.42	5.63	${}^5_{\Lambda}\text{He}$ 3.12(2)
${}^{13}_{\Lambda}\text{C}$ $s_{1/2}$	12.33	11.01	10.54	10.93	4.44	2.24	3.72	8.91	13.40	8.91	6.42	7.22	10.81	14.98	${}^{13}_{\Lambda}\text{C}$ 11.69(12)
$p_{3/2}$	—	—	—	—	—	—	—	—	1.22	—	—	—	0.12	1.76	0.8(3) (p)
$p_{1/2}$	1.11	0.58	0.45	0.72	—	—	—	—	0.97	—	—	—	—	1.40	
${}^{17}_{\Lambda}\text{O}$ $s_{1/2}$	16.12	14.64	14.13	14.65	6.07	3.46	5.35	10.51	16.37	11.46	8.61	9.55	13.60	18.18	${}^{16}_{\Lambda}\text{O}$ 13.0(2)
$p_{3/2}$	3.16	2.29	2.02	2.30	—	—	—	1.22	4.04	1.26	0.14	0.53	2.40	4.89	2.5(2) (p)
$p_{1/2}$	3.47	2.64	2.41	2.76	—	—	—	0.66	3.31	0.51	—	—	1.69	4.10	
${}^{41}_{\Lambda}\text{Ca}$ $s_{1/2}$	24.83	23.17	22.66	23.26	12.37	8.78	11.24	17.56	24.36	19.51	15.86	16.80	21.30	26.47	${}^{40}_{\Lambda}\text{Ca}$ 18.7(1.1) [†]
$p_{3/2}$	14.50	13.05	12.54	12.95	4.95	2.54	3.98	8.82	13.43	9.91	6.93	7.48	11.04	15.06	11.0(5) (p)
$p_{1/2}$	14.70	13.28	12.81	13.25	4.37	2.08	3.50	7.73	12.87	9.13	6.23	6.82	10.42	14.47	
$d_{5/2}$	4.61	3.45	3.01	3.23	—	—	—	0.40	3.59	1.47	—	—	1.99	4.67	1.0(5) (d)
$d_{3/2}$	6.91	5.64	5.18	5.51	—	—	—	0.50	4.02	0.56	—	—	1.20	3.84	
${}^{91}_{\Lambda}\text{Zr}$ $s_{1/2}$	31.27	29.22	28.48	29.11	19.36	14.66	17.83	25.10	32.50	27.72	22.57	23.19	28.94	34.61	${}^{89}_{\Lambda}\text{Y}$ 23.6(5)
$p_{3/2}$	24.31	22.43	21.72	22.22	14.24	10.59	13.27	19.27	25.45	20.59	16.24	16.94	22.05	26.96	17.7(6) (p)
$p_{1/2}$	24.80	22.96	22.28	22.80	13.95	10.39	13.05	19.07	25.31	20.45	15.96	16.67	21.86	26.82	
$d_{5/2}$	16.60	14.79	14.09	14.30	6.21	3.33	5.24	10.30	15.27	11.92	8.10	8.44	12.68	16.78	10.9(6) (d)
$d_{3/2}$	17.57	15.80	15.06	15.40	5.80	2.98	4.88	9.70	14.97	11.65	7.61	7.98	12.27	16.40	
$f_{7/2}$	8.69	7.04	6.25	6.36	—	—	—	1.68	5.63	4.04	0.98	0.89	3.97	7.04	3.7(6) (f)
$f_{5/2}$	10.17	8.58	7.85	8.04	—	—	—	1.28	5.23	3.59	0.33	0.28	3.39	6.54	
${}^{209}_{\Lambda}\text{Pb}$ $s_{1/2}$	40.97	38.18	36.91	37.32	25.75	21.41	25.09	32.28	39.51	36.28	29.50	29.60	35.84	41.58	${}^{208}_{\Lambda}\text{Pb}$ 26.9(8)
$p_{3/2}$	37.62	34.85	33.42	33.50	21.88	15.77	18.33	25.13	31.83	33.72	26.73	25.27	30.26	34.71	22.5(6) (p)
$p_{1/2}$	37.81	35.05	33.62	33.69	21.55	15.53	18.14	25.00	31.74	33.58	26.57	25.13	30.17	34.64	
$d_{5/2}$	29.57	26.94	25.45	25.29	14.47	8.79	9.96	14.78	19.98	25.49	19.28	16.84	20.08	23.15	17.4(7) (d)
$d_{3/2}$	30.03	27.44	26.00	25.87	14.35	8.71	9.83	14.62	19.83	25.29	18.98	16.57	19.85	22.97	
$f_{7/2}$	22.85	20.33	18.92	18.79	4.46	—	—	5.91	12.57	16.23	10.15	7.91	11.90	15.80	12.3(6) (f)
$f_{5/2}$	23.45	20.95	19.57	19.48	4.42	—	—	5.60	12.24	15.96	9.70	7.47	11.47	15.38	
$g_{9/2}$	20.33	17.75	16.23	15.96	1.87	—	—	3.23	9.21	13.72	7.55	5.18	8.92	12.32	7.2(6) (g)
$g_{7/2}$	21.47	18.96	17.50	17.29	1.38	—	—	2.91	8.94	13.38	7.03	4.69	8.53	12.00	
$-U_{\Lambda}(k=0)$	38.75	37.31	36.22	35.62	31.47	26.20	25.22	27.44	28.50	40.99	38.67	35.43	33.76	32.25	27 – 30

Table 1. Separation energies of Λ single-particle states (in MeV) of several hypernuclei from ${}^5_{\Lambda}\text{He}$ to ${}^{209}_{\Lambda}\text{Pb}$, and the BHF Λ single-particle potential at zero momentum, $-U_{\Lambda}(k=0)$, in symmetric nuclear matter at saturation density ($\rho_0 = 0.17 \text{ fm}^{-3}$). Results are shown for the chiral YN interactions at LO [53] and NLO [54, 55] for different values of the cutoff Λ . Available experimental data [1, 73] for the closest measured hypernuclei are included. [†]The weak signal for ${}^{40}_{\Lambda}\text{Ca}$ [74] is not included in the recent compilation [1].

LO interaction agree within 200 keV with those from a Faddeev-Yakubovsky calculation [57].) In Ref. [62] a separation energy of around 4.4 – 4.7 MeV was reported for ${}^5_{\Lambda}\text{He}$ and 13.5 – 14.5 MeV for ${}^{13}_{\Lambda}\text{C}$, for the LO interaction with cutoff $\Lambda = 700$ MeV. These values differ from our predictions by about 1 MeV for the former and by roughly 3 MeV for the latter hypernucleus, cf. Table 1. Thus, taking the results of Wirth and Roth [62] as guideline for what should be the “true” values for the LO interaction, one can conclude that the approach we follow could underestimate the actual values of the binding en-

ergies of light hypernuclei by 20 to 30%. In any case, the Λ single-particle energies for the other hypernuclei calculated with the LO potential, specially for the heavier ones ${}^{91}_{\Lambda}\text{Zr}$ and ${}^{209}_{\Lambda}\text{Pb}$, appear clearly overbound with respect to the experimental values, cf. Table 1. This overbinding is also observed in the BHF result of the Λ single-particle potential in symmetric nuclear matter, $U_{\Lambda}(k=0)$, at the saturation density of $\rho_0 = 0.17 \text{ fm}^{-3}$ which is predicted to be deeper than expected from the analysis of hypernuclear data, see last line of Table 1, indicating that the

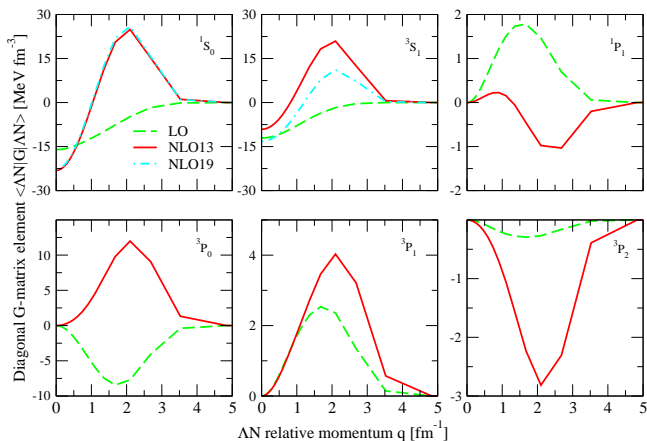


Fig. 2. S - and P -wave diagonal $\Lambda N \rightarrow \Lambda N$ nuclear matter G -matrices as a function of the ΛN relative momentum. Results are shown for the LO (dashed line), NLO13 (solid line) and NLO19 (dash-dotted line) potentials with a cutoff of 600 MeV. The potentials NLO13 and NLO19 yield practically identical G -matrices for P - and higher order waves.

YN G -matrices obtained with chiral interactions at LO are too attractive.

The NLO interactions, and specifically the NLO13 version, predict less bound Λ single-particle states. In particular, there is an underbinding of light hypernuclei such as ${}^5_\Lambda\text{He}$ and ${}^{13}_\Lambda\text{C}$ while the description of the medium and heavier hypernuclei is clearly improved, cf. Table 1. Apparently, neither the NLO13 interaction nor the NLO19 version yield a quantitative description of all medium and heavy hypernuclei. Whereas the NLO19 interaction describes reasonably well ${}^{17}_\Lambda\text{O}$, ${}^{41}_\Lambda\text{Ca}$ and ${}^{91}_\Lambda\text{Zr}$, it seems to overbind ${}^{209}_\Lambda\text{Pb}$. For the latter the predictions of the NLO13 potential are more in line with the experiment. We want to emphasize, however, that in view of the limitations pointed out in Sec. 2, results of the employed approach for heavy hypernuclei such as ${}^{209}_\Lambda\text{Pb}$ are questionable. Indeed, the limitations are evident from Table 1 where one can see that the separation energy for that hypernucleus is sometimes larger than the corresponding value for $U_\Lambda(k=0)$ at nuclear matter saturation density.

To elucidate this reduction of binding when going from LO to NLO we present in Fig. 2 results for selected S - and P -wave diagonal $\Lambda N \rightarrow \Lambda N$ nuclear matter G -matrices as a function of the Λ -nucleon relative momentum. The G -matrices are calculated using the LO, NLO13 and NLO19 potentials, exemplary for a cutoff of 600 MeV. They are evaluated at nuclear matter saturation density $\rho_0 = 0.17 \text{ fm}^{-3}$, zero center-of-mass momentum and a value of the starting energy $\Omega = m_N + m_\Lambda - 80 \text{ MeV}$, where -80 MeV is an average value of the sum of the single-particle mean fields of the nucleon ($U_N(k=k_F) \approx -50 \text{ MeV}$) and the Λ ($U_\Lambda(k=0) \approx -30 \text{ MeV}$) at this density. We remind that the NLO13 and NLO19 potentials differ only in the S -wave channels [55]. It is clear from the figure that the ΛN G -matrices are, overall, less attractive for the NLO interaction than at LO. Specifically, regarding the deci-

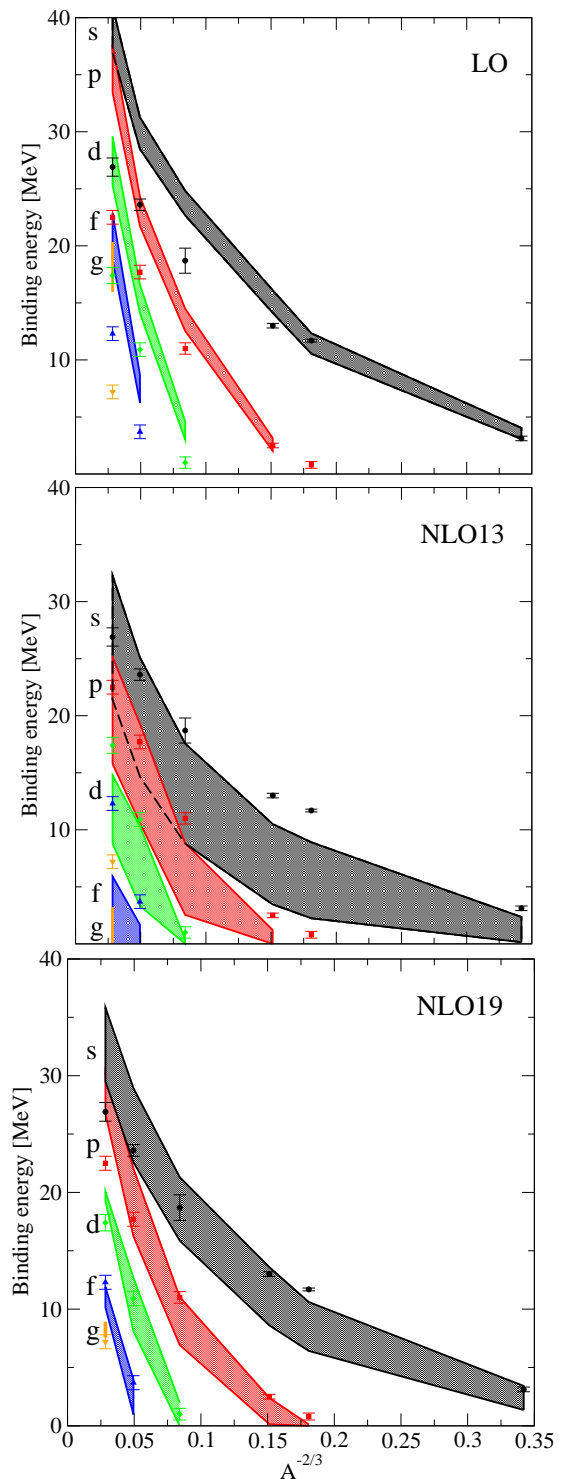


Fig. 3. Energy levels of the $1s$, $1p$, $1d$, $1f$, and $1g$ Λ single-particle shells as a function of $A^{-2/3}$, where A is the baryon number of the hypernucleus defined as $A=N+Z+1$. Theoretical predictions are shown by bands for guiding the eye. The actual calculations were done only for the hypernuclei listed in Table 1. The symbols represent experimental results [1, 73].

sive 1S_0 and 3S_1 partial waves, for the NLO potentials these are attractive (negative) only for small ΛN relative momenta q but change sign, *i.e.* become repulsive, with

increasing momentum. Differences in the AN G -matrices obtained with LO and NLO potentials for the higher partial waves are found to be less than 1 MeV fm^{-3} . Note that the aforementioned differences in the properties of the LO and NLO interactions are also reflected in the corresponding Ap phase shifts presented in Ref. [54].

A graphic representation of our results is provided in Fig. 3. Here bands are shown to guide the eye, where the width represents the variation with the cutoff [54, 55]. This facilitates a more direct view on the regulator dependence. As said above, those variations can be interpreted as a lower bound for the uncertainty of the results due to the truncation of the chiral expansion. Note that a more realistic way for estimating this uncertainty, that does not rely on cutoff variation, has been proposed in Refs. [77]. However, it is not easily applicable to the present calculation.

Figure 3 unveils that the cutoff dependence of the predicted binding energies is sizable. Of course, considering the corresponding variation for the Λ binding in infinite nuclear matter [55, 64, 65], it does not really come unexpectedly. Indeed, like for infinite nuclear matter, the variations at NLO are somewhat larger than the ones at LO – contrary to the trend for YN scattering in free space [54, 55] and for the binding energies of light hypernuclei [55, 57]. In this context we want to mention that a likewise strong regulator dependence has been detected in corresponding studies of nuclear matter properties in the NN sector within chiral EFT [78–81]. As discussed in Ref. [55], since the Pauli operator suppresses the contributions from low momenta, see Eq. (10) of Ref. [44], the G -matrix results are more sensitive to high-momentum contributions and, thus, to intermediate and short-distance physics [80]. In the NN case, indications for a convergence and a reduced regulator dependence were only found after going to much higher order – $N^3\text{LO}$ in Refs. [78, 79] and $N^4\text{LO}$ in [80] – and after including three-body forces. Thus, we anticipate a noticeable reduction of regulator artifacts in the hyperon sector only when 3BFs are explicitly included. This, however, is beyond the scope of the present work as it requires an extension of the YN interaction to at least $N^2\text{LO}$ [56].

Taking the sizable cutoff dependence into account, the predictions of the chiral YN interactions are roughly in line with the experimental information. In case of the NLO19 interaction there is actually a quantitative agreement with the data over an extended range of A values when considering the uncertainty due to the cutoff dependence. Only the heaviest hypernucleus studied, $^{209}_{\Lambda}\text{Pb}$, appears overbound. For the LO (NLO13) interactions we observe a more general tendency for overbinding (underbinding). Looking more carefully on the overall trend one has to conclude that the A dependence predicted by the YN interactions from chiral EFT is definitely somewhat stronger than the one exhibited by the data, see Fig. 3. The very same trend was observed in the earlier studies of s -shell hypernuclei with phenomenological YN interactions, within the same framework [40, 41, 44]. Thus, most likely, one sees here limitations of the employed approach.

Indeed, on the one hand, the method seems to underestimate the binding energies for light hypernuclei, as indicated by the LO predictions for $^5_{\Lambda}\text{He}$ and $^{13}_{\Lambda}\text{C}$ in comparison to results of *ab initio* calculations [62], cf. the discussion above. On the other hand, it overestimates the energies of very heavy hypernuclei as discussed in Sec. 2. Of course, in principle it could be also an indication for (missing) 3BFs. Those appear at higher order and, therefore, are not taken into account in our calculation. Such 3BFs are known to lead to an effective and density-dependent AN interaction [82].

An issue often discussed in the literature is the Λ -nucleus spin-orbit interaction where empirical information suggests that it should be rather weak [1, 2]. It is interesting to see, cf. Table 1, that the splitting of the p -, d -, f - and g -wave states is of the order of few tenths of an MeV or even less in all cases, asserting indeed a small spin-orbit strength of the chiral YN interactions. As a matter of facts, the spin-orbit splittings for the phenomenological YN potentials of the Jülich and Nijmegen groups considered in Refs. [40, 41, 44] were found to be likewise small. Thus, it seems that this feature is well reproduced qualitatively and almost universally by interactions that incorporate the underlying approximate $SU(3)$ symmetry and describe the YN data.

Very prominent cases are the splittings of the $5/2^+$ and $3/2^+$ states of $^9_{\Lambda}\text{Be}$ and of the $3/2^-$ and $1/2^-$ states of $^{13}_{\Lambda}\text{C}$ which are known experimentally with unprecedented accuracy [83, 84]. The ones for $^{13}_{\Lambda}\text{C}$ can be calculated within our approach. However, it turns out that these states are only bound for the NLO interactions and only for the cutoff $\Lambda = 700 \text{ MeV}$, see Table 1. This is already outside of the range of $500 - 650 \text{ MeV}$ considered for the NLO interactions in Refs. [54, 55], guided by the achieved χ^2 values. Since the χ^2 deteriorates only slightly for the larger cutoff – it is 17.3 for NLO13 [54] and 16.5 for NLO19 – we believe, nonetheless, that it is instructive and sensible to take a closer look at the predicted level splitting for the $^{13}_{\Lambda}\text{C}$, even if we have only results for the NLO interactions at $\Lambda = 700 \text{ MeV}$. Certainly, in this case a direct assessment of the cutoff dependence and, accordingly, of the uncertainty is not possible. But it is reassuring to see from the results for heavier hypernuclei that the excitation energies, *i.e.* the difference between the s and p states, are significantly less cutoff dependent. That dependence is even further reduced when the splitting between the $3/2^-$ and $1/2^-$ states itself is considered.

The corresponding results are summarized in Table 2 and compared with the BNL experiment [83]. For the ease of comparison we include in addition the prediction of one of the Nijmegen NSC97 potentials, taken from Ref. [44]. One can see that the measured excitation energies for the $3/2^-$ and $1/2^-$ states are overestimated by about 1 MeV. The splitting of the states is, however, reproduced within 50 keV by the NLO13 interaction considering the experimental uncertainty. The results for the NLO19 interaction and the NSC97e potential are somewhat larger but still remarkably close to the experiment.

	NLO13	NLO13+ALS	NLO19	NLO19+ALS	NSC97e [44]	Exp. [83]
$p_{1/2}$	12.43	12.37	13.58	13.51	12.63	10.982 ± 0.031
$p_{3/2}$	12.18	12.54	13.22	13.63	12.28	10.830 ± 0.031
Δp	0.25	-0.17	0.36	-0.12	0.35	$0.152 \pm 0.054 \pm 0.036$

Table 2. Excitation energies of $^{13}_{\Lambda}\text{C}$ (in MeV) for the chiral YN interactions and the Nijmegen NSC97e potential. Δp denotes the difference $p_{1/2} - p_{3/2}$. ALS indicates that an antisymmetric spin-orbit force was added to the YN potential [64], see text for details.

In Table 2 we show also results for a modified chiral YN potential that was introduced in Ref. [64]. In that work an antisymmetric spin-orbit force (ALS) was added to the NLO interaction from Ref. [54] in an attempt to study its influence on the in-medium properties of the Λ . It is generated by a contact term that facilitates 1P_1 - 3P_1 transitions in the coupled (isospin $I = 1/2$) ΛN - ΣN system. Such a term arises at NLO in the Weinberg counting [54], but it was simply put to zero in the NLO13 interaction because it could not be pinned down by a fit to the existing ΛN and ΣN scattering data. In Ref. [64] this contact term was included and the strength of the corresponding LEC was fixed by considering the so-called Scheerbaum factor S_{Λ} [85] for the Λ calculated in nuclear matter. The Scheerbaum factor provides a measure for the strength of the Λ -nuclear spin-orbit force [63, 86] and values for it have been inferred, *e.g.*, from studies of the splitting of the $5/2^+$ and $3/2^+$ states of $^9_{\Lambda}\text{Be}$ by Hiyama *et al.* [87] and Fujiwara *et al.* [88]. To be concrete, the LEC in question was adjusted to yield $S_{\Lambda} \approx -3.7$, cf. Ref. [64] for a detailed discussion of the choice, whereas the original NLO13 potential predicts values around -12 . As can be seen from Table 2, that modification has a dramatic consequence for the level splitting, namely it reverses the ordering. Thus, the present study suggests that, for the chiral potentials NLO13 and NLO19, such an antisymmetric spin-orbit force has to be more moderate than the one introduced in [64], motivated by the studies in Refs. [63, 86]. In any case, one has to be aware that the very small level splitting results from an extreme fine-tuning of various ingredients of the YN potential. Thus, given the poor overall constraints on the ΛN interaction in higher partial waves [54] and acknowledging the approximate nature of our many-body approach – and of those applied in pertinent studies by other authors – unambiguous conclusions on such detailed aspects of the YN interaction might be difficult to draw at present.

Finally, it is worth noting that the Scheerbaum factor for the LO interaction is around 3 [64], *i.e.*, likewise small but of opposite sign. The $p_{3/2}$ state of $^{13}_{\Lambda}\text{C}$ is not bound in this case, cf. Table 1, only the $p_{1/2}$ state. Notwithstanding, one can see from the results for $^{17}_{\Lambda}\text{O}$, say, that the level ordering is reversed as compared to the NLO interactions. There are NCSM calculations of $^9_{\Lambda}\text{Be}$ for the LO interaction [60, 62]. They reveal that the splitting of the $5/2^+$ and $3/2^+$ states predicted by that interaction is indeed tiny, as suggested by the experiment. However, the level ordering is wrong with respect to the experiment –

but in line with what we observe in our own calculations for heavier hypernuclei.

4 Summary and Conclusions

In this work we have studied the structure of single- Λ hypernuclei using the chiral YN potentials derived by the Jülich–Bonn–Munich group at LO and NLO in the chiral expansion. Following a perturbative many-body approach we have calculated the Λ self-energy in finite nuclei from which we have determined the different Λ single-particle bound states in various hypernuclei from $^5_{\Lambda}\text{He}$ to $^{209}_{\Lambda}\text{Pb}$. We have presented results for the LO potential [53] and the NLO interactions from 2013 (NLO13) [54] and 2019 (NLO19) [55], respectively.

It turned out that the predictions for the YN interaction at LO are in rather good agreement with the empirical separation energies of light hypernuclei, whereas the Λ single-particle energies of the other hypernuclei, specially those of $^{91}_{\Lambda}\text{Zr}$ and $^{209}_{\Lambda}\text{Pb}$, appear clearly too large with respect to the experimental values. However, the good agreement for light hypernuclei is most likely questionable. Available no-core shell model calculations based on the same LO YN interaction for $^5_{\Lambda}\text{He}$ and $^{13}_{\Lambda}\text{C}$ [62] suggest that our approach underestimates the actual binding energies by 20 to 30% when applied to such light systems. That aspect, together with the overbinding for heavier hypernuclei, provides a strong indication that the LO interaction is too attractive.

Calculations for the NLO interactions, particularly for NLO13, yielded less bound Λ single-particle states. Indeed, for NLO13 we observed an overall tendency for underbinding with respect to the empirical information. The predictions for NLO19 turned out to be in a qualitatively good agreement with the data over a fairly large range of mass number values when considering the uncertainty due to the regulator dependence. Only the heaviest considered hypernucleus, $^{209}_{\Lambda}\text{Pb}$, appears overbound by that interaction. However, one should be rather cautious in drawing conclusions from the latter result. As pointed out already in Refs. [41, 44], and as discussed in the present work as well, there are clear signals for shortcomings of the employed approach when applied to such heavy hypernuclei. In particular, one has to keep in mind that the method itself was originally optimized for the study of $^{17}_{\Lambda}\text{O}$, although it is expected to work also reasonably well for, say, $^{13}_{\Lambda}\text{C}$ and $^{41}_{\Lambda}\text{Ca}$. Independently of that, the sizable regulator depen-

dence is a clear signal that higher-order contributions, and specifically three-body forces, have to play a role.

Finally, the predicted spin-orbit splittings of the p -, d -, f -, and g -wave states are found to be very small. These are of the order of few tenths of MeV or even less, in remarkable agreement with the magnitude observed in experiments. Actually, similarly small values were also obtained in corresponding calculations [44] for meson-exchange YN potentials by the Jülich and Nijmegen groups, thus, corroborating that this feature can be qualitatively well reproduced by interactions that take account of the underlying approximate SU(3) flavor symmetry and describe the Λp and ΣN scattering data.

We acknowledge helpful communications with Avraham Gal, Andreas Nogga and Hirokazu Tamura. This work is partially supported by the COST Action CA16214 and by the DFG and the NSFC through funds provided to the Sino-German CRC 110 ‘‘Symmetries and the Emergence of Structure in QCD’’ (DFG grant. no. TRR 110).

References

1. A. Gal, E. V. Hungerford, and D. J. Millener, *Rev. Mod. Phys.* **88**, 035004 (2016).
2. E. Botta, T. Bressani, and G. Garbarino, *Eur. Phys. J. A* **48**, 41 (2012).
3. O. Hashimoto and H. Tamura, *Prog. Part. Nucl. Phys.* **57**, 564 (2006).
4. R. Engelmann, H. Filthuth, V. Hepp, and E. Kluge, *Phys. Rev. Lett.* **21**, 587 (1966).
5. G. Alexander, U. Karshon, A. Shapira, G. Yekutieli, R. Engelmann, F. Filthuth, and W. Lughofer, *Phys. Rev.* **173**, 1452 (1968).
6. B. Sechi-Zorn, B. Kehoe, J. Twitty, and R. A. Burnstein, *Phys. Rev.* **175**, 1735 (1968).
7. J. A. Kadyk, G. Alexander, J. H. Chan, P. Gaposchkin, and G. H. Trilling, *Nucl. Phys. B* **27**, 13 (1971).
8. A. Bouyssy and J. Hüfner, *Phys. Lett. B* **64**, 276 (1976).
9. A. Bouyssy, *Phys. Lett. B* **84**, 41 (1979).
10. C. D. Dover, L. Ludeking, and G. E. Walker, *Phys. Rev. C* **22**, 2073 (1980).
11. T. Motoba, H. Bandō, R. Wünsch and J. Žofka *Phys. Rev. C* **38**, 1322 (1988).
12. D. J. Millener, C. B. Dover and A. Gal, *Phys. Rev. C* **38**, 2700 (1988).
13. Y. Yamamoto, H. Bandō and J. Žofka, *Prog. Theor. Phys.* **80**, 757 (1988).
14. F. Fernández, T. López-Arias and C. Prieto, *Z. Phys. A* **334**, 349 (1989).
15. D. E. Lanskoy and Y. Yamamoto, *Phys. Rev. C* **55**, 2330 (1997).
16. T. Y. Tretyakova and D. E. Lanskoy, *Eur. Phys. J. A* **5**, 391 (1999).
17. J. Cugnon, A. Lejeune, and H.-J. Schulze, *Phys. Rev. C* **62**, 064308 (2000).
18. I. Vidaña, A. Polls, A. Ramos and H.-J. Schulze, *Phys. Rev. C* **64**, 044301 (2001).
19. X.-R. Zhou, H.-J. Schulze, H. Sagawa, C.-X. Wu and E.-G. Zhao, *Phys. Rev. C* **76**, 034312 (2007).
20. X.-R. Zhou, A. Polls, H.-J. Schulze and I. Vidaña, *Phys. Rev. C* **78**, 054306 (2008).
21. R. Brockmann and W. Weise, *Nucl. Phys. A* **355**, 365 (1981).
22. M. Chiapparini, A. O. Gattone and B. K. Jennings, *Nucl. Phys. A* **529**, 589 (1991).
23. J. Boguta and S. Bohrmann, *Phys. Lett. B* **102**, 93 (1981).
24. J. Mareš and J. Žofka, *Z. Phys. A* **333**, 209 (1989).
25. N. K. Glendenning, D. Von-Eiff, M. Haft, H. Lenske and M. K. Weigel, *Phys. Rev. C* **48**, 889 (1993).
26. J. Mareš and B. K. Jennings, *Phys. Rev. C* **49**, 2472 (1994).
27. Y. Sugahara and H. Toki, *Prog. Theor. Phys.* **92**, 803 (1994).
28. R. J. Lombard, S. Marcos and J. Mareš, *Phys. Rev. C* **51**, 1784 (1995).
29. Z. Ma, J. Speth, S. Krewald, B. Chen and A. Reuber, *Nucl. Phys. A* **608**, 305 (1996).
30. F. Ineichen, D. Von-Eiff and M. K. Weigel, *J. Phys. G* **22**, 1421 (1996).
31. K. Tsushima, K. Saito and A. W. Thomas, *Phys. Lett. B* **411**, 9 (1997).
32. K. Tsushima, K. Saito, J. Haidenbauer and A. W. Thomas, *Nucl. Phys. A* **630**, 691 (1998).
33. E. N. E. van Dalen, G. Colucci and A. Sedrakian, *Phys. Lett. B* **734**, 383 (2014).
34. Y. Yamamoto and H. Bandō, *Prog. Theor. Phys. Suppl.* **81**, 9 (1985).
35. Y. Yamamoto and H. Bandō, *Prog. Theor. Phys.* **83**, 254 (1990).
36. Y. Yamamoto, J. Reuber, H. Himeno, S. Nagata and T. Motoba, *Czech. J. Phys.* **42**, 1249 (1992).
37. Y. Yamamoto, T. Motoba, H. Himeno, K. Ikeda and S. Nagata, *Prog. Theor. Phys. Suppl.* **117**, 361 (1994).
38. D. Halderson, *Phys. Rev. C* **48**, 581 (1993).
39. J. Hao, T. T. S. Kuo, A. Reuber, K. Holinde, J. Speth and D. J. Millener, *Phys. Rev. Lett.* **71**, 1498 (1993).
40. M. Hjorth-Jensen, A. Polls, A. Ramos and H. Müther, *Nucl. Phys. A* **605**, 458 (1996).
41. I. Vidaña, A. Polls, A. Ramos and M. Hjorth-Jensen, *Nucl. Phys. A* **644**, 201 (1998).
42. D. Lonardoni, S. Gandolfi and F. Pederiva, *Phys. Rev. C* **87**, 041303 (R) (2013).
43. D. Lonardoni, F. Pederiva and S. Gandolfi, *Phys. Rev. C* **89**, 014314 (2014).
44. I. Vidaña, *Nucl. Phys. A* **958**, 48 (2017).
45. B. Holzenkamp, K. Holinde and J. Speth, *Nucl. Phys. A* **500**, 485 (1989).
46. J. Haidenbauer and U.-G. Meißner, *Phys. Rev. C* **72**, 044005 (2005).
47. P. M. M. Maesen, Th. A. Rijken and J. J. de Swart, *Phys. Rev. C* **40**, 2226 (1989).
48. Th. A. Rijken, V. G. J. Stoks and Y. Yamamoto, *Phys. Rev. C* **59**, 21 (1999).

49. V. G. J. Stoks and Th. A. Rijken, *Phys. Rev. C* **59**, 3009 (1999).
50. Th. A. Rijken and Y. Yamamoto, *Phys. Rev. C* **73**, 044008 (2006).
51. Th. A. Rijken, M. M. Nagels and Y. Yamamoto, *Prog. Theor. Phys. Suppl.* **185**, 14 (2010).
52. M. M. Nagels, T. A. Rijken and Y. Yamamoto, *Phys. Rev. C* **99**, 044003 (2019).
53. H. Polinder, J. Haidenbauer, and U.-G. Meißner, *Nucl. Phys. A* **779**, 244 (2006).
54. J. Haidenbauer, S. Petschauer, N. Kaiser, U.-G. Meißner, A. Nogga, and W. Weise, *Nucl. Phys. A* **915**, 24 (2013).
55. J. Haidenbauer, U.-G. Meißner, and A. Nogga, arXiv:1906.11681.
56. S. Petschauer, N. Kaiser, J. Haidenbauer, U.-G. Meißner and W. Weise, *Phys. Rev. C* **93**, 014001 (2016).
57. A. Nogga, *Nucl. Phys. A* **914**, 140 (2013).
58. R. Wirth, D. Gazda, P. Navrátil, A. Calci, J. Langhammer and R. Roth, *Phys. Rev. Lett.* **113**, 192502 (2014).
59. D. Gazda and A. Gal, *Phys. Rev. Lett.* **116**, 122501 (2016).
60. R. Wirth and R. Roth, *Phys. Rev. Lett.* **117**, 182501 (2016).
61. D. Gazda and A. Gal, *Nucl. Phys. A* **954**, 161 (2016).
62. R. Wirth and R. Roth, arXiv:1902.03324 [nucl-th].
63. M. Kohno, *Phys. Rev. C* **81**, 014003 (2010).
64. J. Haidenbauer and U.-G. Meißner, *Nucl. Phys. A* **936**, 29 (2015).
65. S. Petschauer, J. Haidenbauer, U.-G. Meißner, and W. Weise, *Eur. Phys. J. A* **52**, 15 (2016).
66. J. Haidenbauer, U.-G. Meißner, N. Kaiser, and W. Weise, *Eur. Phys. J. A* **53**, 121 (2017).
67. M. Kohno, *Phys. Rev. C* **97**, 035206 (2018).
68. D. Chatterjee and I. Vidaña, *Eur. Phys. J. A* **52**, 29 (2016).
69. A. Nogga, *AIP Conf. Proc.* **2130**, 030004 (2019).
70. H. Le, J. Haidenbauer, U.-G. Meißner and A. Nogga, arXiv:1909.02882 [nucl-th].
71. M. Borromeo, D. Bonatsos, H. Müther and A. Polls, *Nucl. Phys. A* **539**, 189 (1992).
72. M. Hjorth-Jensen, H. Müther and A. Polls, *Phys. Rev. C* **50**, 501 (1994).
73. E. Botta, T. Bressani and A. Feliciello, *Nucl. Phys. A* **960**, 165 (2017).
74. P. H. Pile *et al.*, *Phys. Rev. Lett.* **66**, 2585 (1991).
75. E. Epelbaum, H.-W. Hammer and U.-G. Meißner, *Rev. Mod. Phys.* **81**, 1773 (2009).
76. H. W. Hammer, A. Nogga and A. Schwenk, *Rev. Mod. Phys.* **85**, 197 (2013).
77. E. Epelbaum, H. Krebs and U.-G. Meißner, *Eur. Phys. J. A* **51**, 53 (2015).
78. L. Coraggio, J. W. Holt, N. Itaco, R. Machleidt and F. Sammarruca, *Phys. Rev. C* **87**, 014322 (2013).
79. F. Sammarruca, L. Coraggio, J. W. Holt, N. Itaco, R. Machleidt and L. E. Marcucci, *Phys. Rev. C* **91**, 054311 (2015).
80. J. Hu, Y. Zhang, E. Epelbaum, U.-G. Meißner and J. Meng, *Phys. Rev. C* **96**, 034307 (2017).
81. J. Hu, P. Wei and Y. Zhang, arXiv:1909.11826 [nucl-th].
82. S. Petschauer, J. Haidenbauer, N. Kaiser, U.-G. Meißner and W. Weise, *Nucl. Phys. A* **957**, 347 (2017).
83. H. Kohri *et al.* [AGS-E929 Collaboration], *Phys. Rev. C* **65**, 034607 (2002).
84. H. Akikawa *et al.*, *Phys. Rev. Lett.* **88**, 082501 (2002).
85. R. R. Scheerbaum, *Nucl. Phys. A* **257**, 77 (1976).
86. Y. Fujiwara, M. Kohno, T. Fujita, C. Nakamoto and Y. Suzuki, *Nucl. Phys. A* **674**, 493 (2000).
87. E. Hiyama, M. Kamimura, T. Motoba, T. Yamada and Y. Yamamoto, *Phys. Rev. Lett.* **85**, 270 (2000).
88. Y. Fujiwara, M. Kohno, K. Miyagawa and Y. Suzuki, *Phys. Rev. C* **70**, 047002 (2004).